

Quantifying sediment storage on the floodplains outside levees along the lower Yellow River during the years 1580–1849

Yunzhen Chen,^{1,2*}  Irina Overeem,³ Albert J. Kettner,³ Shu Gao,⁴ James P. M. Syvitski³ and Yuanjian Wang⁵

¹ School of Marine Science, Sun Yat-sen University, Guangzhou 510275, China

² Guangdong Provincial Key Laboratory of Marine Resources and Coastal Engineering, Guangzhou, China

³ CSDMS/INSTAAR, University of Colorado Boulder, Boulder, Colorado USA

⁴ State Key Laboratory for Estuarine and Coastal Studies, East China Normal University, Shanghai, China

⁵ Yellow River Institute of Hydraulic Research, Zhengzhou, Henan China

Received 15 July 2017; Revised 19 September 2018; Accepted 20 September 2018

*Correspondence to: Yunzhen Chen, School of Marine Science, Sun Yat-sen University, Guangzhou, 510275, China. E-mail: chenyzh49@mail.sysu.edu.cn



ABSTRACT: The lower Yellow River channel was maintained by artificial levees between 1580 and 1849. During this period, 280 levee breaches occurred. To estimate sediment storage on the floodplains outside the levees, a regression model with a decadal time step was developed to calculate the outflow ratio for the years when levee breaching occurred. Uncertainty analysis was used to identify the likely outflow ratio. Key variables of the model include annual water discharge, a proxy for levee conditions, and potential bankfull discharge of the channel before flood season. Uncertainty analysis reveals an outflow ratio of 0.35–0.56. We estimate that during this period, 18.8–30.1% of the total ~312 Gt of sediment load was deposited on the floodplains outside the levees. Human-accelerated erosion in the Loess Plateau caused a 4-fold increase in sediment delivery to the lower Yellow River, which could not be accommodated by channel morphodynamic changes. As a result, 21.2–27.5% of the total sediment load was deposited within the levees, creating a super-elevated channel bed that facilitated an unusually high breach outflow ratio. Hence, the factor of a large super-elevation relative to the mean main channel depth should be considered when designing diversions to restore floodplains. © 2018 John Wiley & Sons, Ltd.

KEYWORDS: Sediment budget; Yellow River; Levee breaches; Floodplain sedimentation; Bankfull discharge

Introduction

Rivers are sediment transport features in the landscape that run from a source to the coastal ocean (Allen, 2008; Bracken *et al.*, 2015). In alluvial rivers, a significant fraction of the sediment eroded within a drainage basin is deposited within its channel belts, floodplains or wetlands, often outside the levees, rather than being delivered to an ocean (Walling, 1983; Milliman and Syvitski, 1992; Allison *et al.*, 1998; Dunne *et al.*, 1998; Goodbred and Kuehl, 1999). Since pre-industrial times, through changing land use and levee construction, humans have unintentionally affected sediment fluxes through river systems, resulting in substantial modifications to the geomorphic evolution of rivers, floodplains and receiving coastal zones (Wolman, 1967; Kesel, 1988; Gregory, 2006; Walling, 2006; Syvitski and Kettner, 2011; Pietsch *et al.*, 2015; Bergillos *et al.*, 2016; Lewin *et al.*, 2017). By managing intentional levee breaks or engineered diversion structures, modern societies are purposefully affecting sediment fluxes through river systems for the sake of building land or restoring floodplain ecosystems (Florsheim and Mount, 2002; Wang *et al.*, 2003; Florsheim and Dettinger, 2015; Kesel and McGraw, 2015; Ollero *et al.*, 2015).

The Rhine Delta was an efficient sediment trap before an embankment was constructed between 1100 and 1300 AD. As of today, 94.4% of the total floodplain area has been cut off by levees from overbank sedimentation. As a result, only ~13% of the sediment delivered to the delta can be trapped by the embanked floodplains (Middelkoop *et al.*, 2010).

On the lower Mississippi River, since 1927, little sediment has been stored in the floodplains outside the levees, as the levee system was upgraded to prevent overbank flooding and crevassing (Kesel *et al.*, 1992; Kesel, 2003). Notable coastal wetland losses have subsequently occurred over the last century (Kesel, 1989; Day *et al.*, 2007). To rebuild these wetlands, diversion structures are being used to deliver sediment and freshwater to the surrounding wetland areas (Kesel and McGraw, 2015; Meselhe *et al.*, 2016; Esposito *et al.*, 2017).

The lower Yellow River is an ideal area for studying the impacts of human activities, particularly the impact of embankments, on floodplain sedimentation processes. The Yellow River is a large river system in terms of sediment loads and the area of its alluvial plain. In the early 20th century, the annual average sediment load of the lower Yellow River reached 1.6 Gt (Ren, 2015). The extensive alluvial plain covers an area of ~250,000 km² (Figure 1). Historically, the lower Yellow River

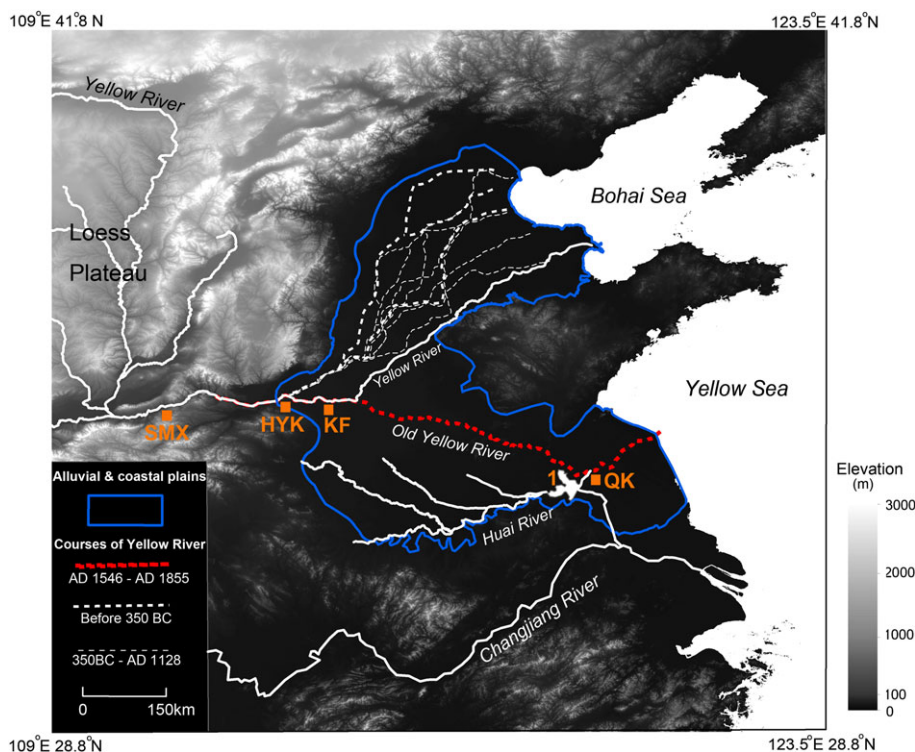


Figure 1. Study area showing that the lower Yellow River changed its course numerous times throughout history and discharged into the Bohai or Yellow Sea and that it had an extensive $\sim 250,000 \text{ km}^2$ alluvial plain. During AD 1578–1855, the lower Yellow River channel was maintained in the Old Yellow River by artificial levees. Dammed by the super-elevated channel of the Old Yellow River, the Huai River was forced to flow southward and discharge into the Changjiang River. SMX: Sanmenxia, HYK: Huayankou, KF: Kaifeng, QK: Qingkou, 1: Hongze Lake. [Colour figure can be viewed at wileyonlinelibrary.com]

has shifted its course >30 times, discharging into either the Bohai Sea or Yellow Sea; its levees were breached >1000 times and large volumes of sediment were distributed and deposited on the alluvial plain.

Ninety percent of the sediment supplied to the lower Yellow River originates from the Loess Plateau, which is located in the middle basin (Figure 1). Over two millennia, human-accelerated erosion in the Loess Plateau has caused an estimated 3- to 10-fold increase in sediment load to the lower river (Milliman *et al.*, 1987; Ren and Zhu, 1994; Chen *et al.*, 2015). Over these two millennia, unparalleled resources have been devoted to preventing floods by placing embankments along the lower river. Management climaxed between 1580 and 1849, when the river channel was secured in the Old Yellow River location by an artificial levee system (Figure 1). Humans persisted in repairing levees and in plugging breaches to prevent the Yellow River from shifting its course (Xu, 1993; Chen *et al.*, 2015).

For the Old Yellow River, sediment accumulated within the artificial levees, eventually forming an elevated channel belt $\sim 10 \text{ m}$ higher than its surrounding area (Figure 2). At the same time, large amounts of sediment were bypassing the levees and being deposited on the floodplains as a result of significant and frequent breaches, given the super-elevation of the channel belt and the weakness of the earthen levees (Chen *et al.*, 2015). In 1841, the Yellow River breached its levee close to the city of Kaifeng (Figure 2); the river flowed through this breach for 8 months, depositing a volume of 3 m-thick silt on the floodplains that extended $\sim 8 \text{ km}$ beyond the levees.

The breach events on the Old Yellow River were characterized by a high frequency of outflows of unusually high magnitude and long duration (Shen *et al.*, 1935). Studies on human-influenced sediment flux to the floodplains beyond the levees along the lower Yellow River in historical times offer insight

for assessing the risks of levee breaches, managing intentional levee breaks and engineering diversion structures on rivers.

After embankment, the sediment input to the lower Yellow River from the upper and middle basins could be trapped by three depositional features: 1) the channel belt and floodplains within the artificial levees, 2) the floodplains outside the levees, and 3) the river delta and its associated basin. Ren (2015) estimated that between 1550 and 1855, the annual sediment load for the lower Yellow River was 1.1 Gt, of which 12%, 34% and 54%, respectively, were distributed across the abovementioned depositional features. Ye *et al.* (1983) estimated that from 1494 to 1855, the annual sediment load of the lower Yellow River was 1.3 Gt, of which 44% was sequestered on the first two mentioned depositional features and 56% delivered to the river delta and beyond. These sediment budgets are based on analyses of geomorphological maps of alluvial fans, limited stratigraphic cross sections, sparse core data, comparisons with modern conditions, and expert opinions (Ye *et al.*, 1983; Ren, 2015).

The unconfined and super-elevated lower Yellow River has extensive floodplains (Figures 1 and 2); thus, it is expensive and time-consuming to collect a large amount of stratigraphic data to quantify spatial heterogeneities in floodplain sedimentation. Here, we construct a multiple regression model that determines the decadal-averaged probability of levee breaches to predict sediment flux to the floodplains outside the levees for 1580–1849, which is made possible by the detailed historical records available for this period. Further, we determine the uncertainty range for the prediction and construct a sediment budget for the Old Yellow River. Sediment budgets for other historical periods are also investigated to better understand human impacts on sediment fluxes and their geomorphic consequences from 1580 to 1849.

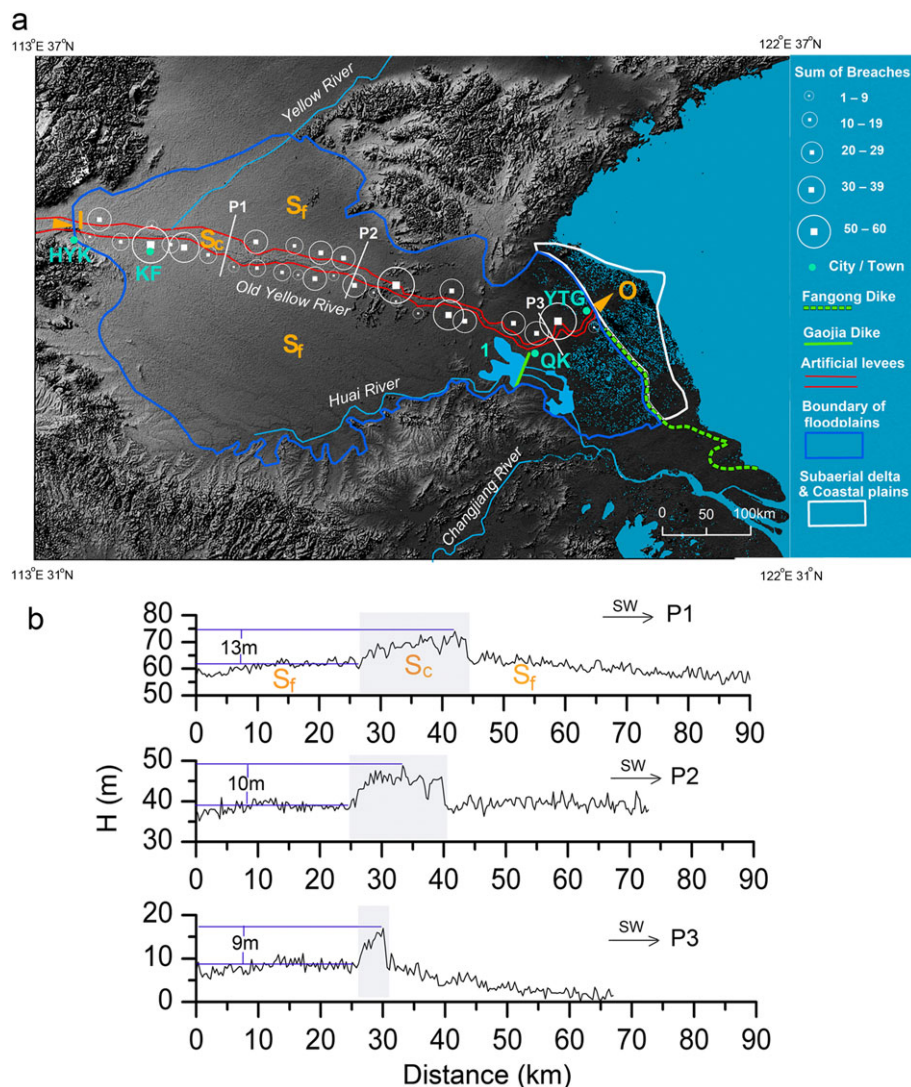


Figure 2. (a) Shuttle Radar Topography Mission (SRTM) 90 m resolution view of the elevation of the abandoned Old Yellow River channel and the approximate boundaries of its active floodplains. The circles show levee breach locations and the sum of breach occurrences at these locations between AD 1580 and 1849. The subaerial delta and coastal plains were created by the Yellow River before it shifted back to the northern plains in 1855. The shoreline is delineated on the basis of a historical map from the 1820s (Tan, 1982). HYK: Huayuankou, KF: Kaifeng, Qk: Qingkou, YTG: Yuntiguan, 1: Hongze Lake. (b) Topographic cross sections based on SRTM 90 m resolution data display remaining deposits of the abandoned channel belt. The four components of the sediment budget are marked in (a) and (b). I is the sediment input to the Old Yellow River at Huayuankou; O is the sediment output at Yuntiguan, the apex of the delta; S_c is the sediment flux deposited in channel belts and floodplains within levees; and S_f is the sediment flux stored in floodplains beyond levees. [Colour figure can be viewed at wileyonlinelibrary.com]

Our model suggests that risks of levee breaches on rivers around the globe can be altered by climate change and human activities in the future, which is addressed in the discussion. We explain why the Old Yellow River, though embanked, still transferred a high ratio of sediment to its floodplains beyond the levees and the implication for managing self-sustainable diversions.

Study Area

Channel Conditions

In 1128, an artificial avulsion allowed the lower Yellow River to capture the Huai River, and for the following 700 years, the Yellow River drained south-eastwards into the Yellow Sea (Xu, 1989). From 1128 to 1577, due to a laissez-faire attitude towards levee breaches, the main course of the Yellow River shifted among tributaries of the Huai River. In 1578–1579, an extensive levee system was constructed along the Bian River, a tributary of the Huai River. As a result, no major avulsions

occurred from 1578 to 1855. In 1855, a northward avulsion diverted the Yellow River back to the North China Plain and Bohai Sea (Chen *et al.*, 2012; Figure 1).

The Old Yellow River, or the lower Yellow River from 1578 to 1855, which includes relic super-elevated channel belts and floodplains within levees that can be easily identified from SRTM imagery, was ~800 km long from the alluvial fan apex close to the Huayuankou gauging station to the apex of the subaerial delta close to Yuntiguan (Figure 2). The distance between the opposing levees decreased from ~14 km upstream to <5 km farther downstream as the river's channel pattern shifted downstream from braided to meandering.

Water and Sediment Discharges

The confluence of the Old Yellow River and the main stream of the Huai River was located at Qingkou, which is positioned approximately 120 km upstream from the delta apex (Figure 2). As the channel bed of the Huai River was much lower than that of the Yellow River, a substantial proportion of Huai River

discharge was forced southward to the Changjiang River or Yellow Sea; only a small portion of the flow was captured by the Yellow River at Qingkou (Pietz, 2002; Figure 2). Therefore, discharge from the Old Yellow River mostly originated from the upper and middle basins of the Yellow River, upstream from Huayuankou.

The mean annual water discharge of the Old Yellow River at Huayuankou was slightly larger than that at Sanmenxia, which was 268 km upstream (Figure 1) and had a long-term annual water discharge of 52 km³ between 1580 and 1849 (Wang *et al.*, 1999). The mean annual sediment discharge of the Old Yellow River at Huayuankou was 1.0–1.3 Gt, as soil erosion in the Loess Plateau was exacerbated by excessive reclamation from 1580 to 1849 (Ye *et al.*, 1983; Shi *et al.*, 2009; Ren, 2015). The median grain size of suspended sediments in the lower Yellow River was 0.02 mm (Chien and Zhou, 1965).

Floods and Landscape Evolution

Long-term sedimentation rates for the channel belt and floodplains within the levees are estimated to have been 20–30 mm yr⁻¹ (Xu, 1998). In the 1850s, before the channel belt of the Old Yellow River was abandoned, its elevation above the adjacent floodplain reached >10 m, as measured from the extracted elevation profiles (Figure 2).

Super-elevated rivers are prone to breach levees. Historical documents show that from AD 1580–AD 1849, the Old Yellow River experienced 280 levee breaches (Supporting Material Table S1). We mapped these levee breach sites onto SRTM 90 m topography images and found that the levee breach sites are evenly distributed along the Old Yellow River (Figure 2). The breaches diverted impressive and long-lasting flows from the main channel. From 1580 to 1849, at least 34 major

breaches resulted in the drying-up of the Yellow River downstream and simultaneously in siltation of the channel downstream. Most breaches were not repaired until the following spring or even longer (Shen *et al.*, 1935; Chen *et al.*, 2015), so that a large amount of water and sediment diverged onto the floodplains outside the levees.

The active floodplains of the Old Yellow River have a total area of ~136,000 km² and can extend 100–200 km from the levees (Figure 2). Stratigraphic data show that the thickness of flood deposits on crevasse splays varies from 1 to 15 m (Chen, 1989; Wu, 1996). Flood deposits consist mainly of silt and clay. The dry bulk density of flood deposits is 1.24–1.70 g cm⁻³ (Ma *et al.*, 1997; Shi *et al.*, 2002).

The Hongze Lake did not exist before the Huai River was captured by the Yellow River in 1128 (Figure 3). The lake developed as the Huai River was dammed by the super-elevated channel belt of the Old Yellow River (Ren, 1992). A subaerial delta started to develop in 1128, and a large amount of sediment discharge was deposited on the coastal plains to the south of the delta (Figure 3; Zhang, 1984; Ren, 1992). Only a small amount of sediment was dispersed into the outer shelf and ocean (Milliman *et al.*, 1989; Ren, 2015).

From 1580 to 1849, 657 levee maintenance and breach closure projects were implemented (Shen *et al.*, 1935). In 1855, the levee system was overwhelmed by a major avulsion event, and the Yellow River shifted to its present course. Since 1950, no levee breaches have occurred upstream of the delta apex.

Methods and Data

Procedure for Prediction

To estimate the amount of sediment that was stored on the floodplains outside the levees from 1580 to 1849, we predict

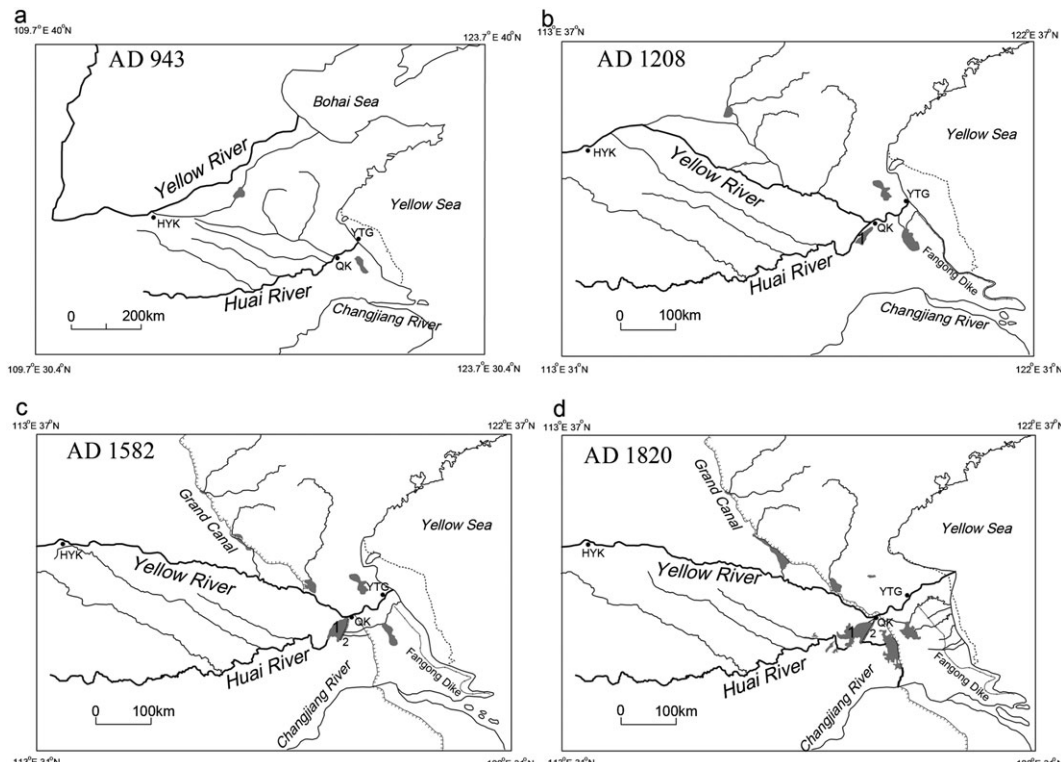


Figure 3. Historical (AD 943, 1208, 1582 and 1820) changes in the course of the lower Yellow River, in the drainage network of the Huai River, in lakes in the floodplains and in coastlines shaped by sediments of the Yellow River on the basis of historical maps shown in (Tan, 1982). HYK: Huayuankou, QK: Qingkou, YTG: Yuntiguan; 1: Hongze Lake, 2: Gaojia Dike. Coastlines shown as dotted lines are current coastlines together with the Fangong Dike built in the 11th century and serve as a frame of reference in terms of coastline changes.

the long-term averaged outflow ratio of breaches for this period (R_o), as S_f is calculated by:

$$S_f \approx R_o I \quad (1)$$

where I is the sediment input to the Old Yellow River at Huayuankou, which is estimated to have been 1.0 to 1.3 Gt yr⁻¹ (Ye et al., 1983; Shi et al., 2009). Here, the outflow ratio for sediment discharge approximates that of water discharge, as the sediment concentration in flows through a breach is close to that in river flows assuming that the bottom of the breach reaches the riverbed. This situation is very likely for the breaches of the super-elevated Old Yellow River. Historical documents record a breach erosion depth as large as 23–27 m during this period (Shen et al., 1935). R_o is calculated as follows:

$$R_o = \frac{\sum_{i=1}^{270} Q_o(i)}{\sum_{i=1}^{270} Q(i)} \quad (2)$$

where $\sum_{i=1}^{270} Q(i)$ is the volume of annual water discharge at Huayuankou from 1580 to 1849, $\sum_{i=1}^{270} Q_o(i)$ is the sum of annual breach outflows for 1580–1849, and i indicates the years from 1580 to 1849. Assuming an annual outflow ratio r_{oa} that is equal for all breach years, $Q_o(i)$ for breach years can be calculated as:

$$Q_o(i) = r_{oa} Q(i) \quad (3)$$

To estimate r_{oa} , we construct a model for the probability of levee breaches on the Yellow River, including r_{oa} as a model parameter. We then apply an automatic calibration that uses an uncertainty analysis to identify its most likely value (Chen et al., 2015). Two additional uncertainty analyses are applied to investigate the full uncertainty range.

Regression Model for the Probability of Levee Breaches

Two key factors affecting the occurrence of a levee breach are 1) the water level above the channel bed (as jointly controlled

by the ratio of water discharge to the bankfull discharge of a channel) and 2) the condition of the levees. We formulate a multi-exponential regression model for the decadal average probability of a levee breach on the Old Yellow River from 1580 to 1849 as follows:

$$P = X_1 \left(\frac{Q}{Q_{bf}} \right)^{X_2} L_v^{X_3} \quad (4)$$

All variables are decadal-averaged time-series either reconstructed from historical observations or calculated using empirical equations, as explained in the following section. P is the annual probability of breach occurrence, Q is the annual water discharge at Huayuankou, L_v is a proxy for levee conditions in a given year, and Q_{bf} is bankfull discharge of the channel before the flood season with its magnitude depending on r_{oa} (see below). X_1 , X_2 and X_3 are model parameters, which are estimated using a least squares fit model and thus vary with r_{oa} .

The data sources used and the construction of variables in Equation (4) are as follows:

P and L_v are based on records from *The Chronicle of the Yellow River* (Shen et al., 1935). All events noted as “breach” and “avulsion” in the written chronology are counted as breach events. The annual probability of breach occurrence for a given year is calculated by dividing the sum of breach events occurring in a given year by 365. Levee construction, maintenance and repair projects are noted as “construction” in the chronicle. We assume earthen levees during this period had a lifetime of T years, and we take the sum of “construction” projects for the previous T years as a proxy for levee conditions in a given year. As the lower Yellow River had been fixed to the course of the Old Yellow River since AD 1546, the sum of “construction” projects is set to 0 for years prior to AD 1546.

T ranges from 10 to 90, and by sampling T at equal intervals of 10, we draw nine discrete likely values for T , that is, $T = \{10, 20, \dots, 80, 90\}$. For every likely value of T , the coefficient of determination (R^2) is calculated to estimate to what extent the decadal sum of breach event occurrence is correlated with T . As R^2 reaches its maximum value 0.29 at $T=40$ (Figure 4), we estimate that earthen levees have a lifetime of 30–50 years.

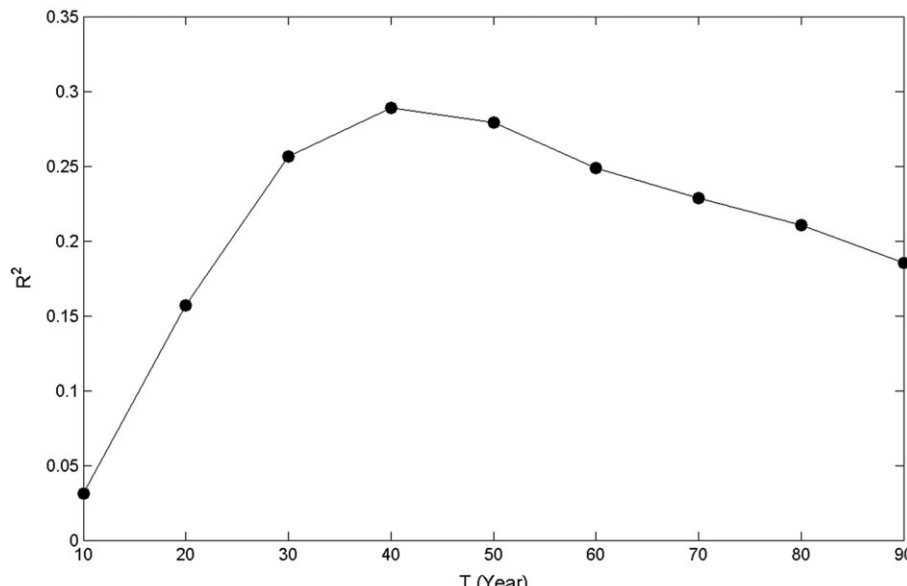


Figure 4. Changes in the correlation between the decadal sum of breach events and the proxy of levee conditions (L_v) with the lifetime of levees (T). The coefficient of determination R^2 peaks at $T=40$, suggesting that earthen levees have a lifetime of ~40 years.

Q is constructed from the time-series of annual discharge at the Sanmenxia station (Figure 1), which is an estimated time-series by Wang *et al.* (1999) using several historical data correlations. Long-term annual water discharge at Huayuankou is approximately 1.1 times that observed at Sanmenxia in modern times. Therefore, annual water discharge at Sanmenxia is multiplied by 1.1 to obtain an estimate of discharge at Huayuankou, which is denoted as Q_a . Averaging Q_a decadally yields Q .

For the lower Yellow River between 1950 and 2003, Chen *et al.* (2006) formulated an empirical relationship between annual water discharge at Huayuankou Q_a and the magnitude of post-flood bankfull discharge for a given year Q_{bfa} :

$$Q_{bfa} = -0.0117Q_a^2 + 20.5Q_a - 733.3 \quad (150 \leq Q_a \leq 876) \quad (5)$$

where the units of Q_a and Q_{bfa} are $0.1 \text{ km}^3 \text{ yr}^{-1}$ and $\text{m}^3 \text{ s}^{-1}$, respectively. We assume that for the Old Yellow River, Q_{bfa} can be calculated similarly using Q_a in a quadratic function but with three coefficients different from those of the current Yellow River.

Our prediction of the three coefficients is based on reasoning as follows: how would the equation for Q_{bfa} of the lower Yellow River from 1950 to 2003 deviate from Equation (5) if there were no human-induced reduction of water discharges during flood seasons. Since the 1960s, river diversion and regulation have significantly reduced water discharges both annually and during flood seasons, particularly the proportion of discharges during flood seasons, resulting in a remarkable narrowing of the channel for the lower Yellow River (Chen *et al.*, 2006; Wang *et al.*, 2007; Wu *et al.*, 2008). The bankfull discharge decreased from 7000 to 8000 $\text{m}^3 \text{ s}^{-1}$ in the 1950s to 2200–2800 $\text{m}^3 \text{ s}^{-1}$ in the 2000s (Chen *et al.*, 2006).

A near-pristine relationship between annual water discharge and post-flood bankfull discharge can be calculated using two equations. One equation is the correlation between water discharge in flood seasons from July to October Q_f ($0.1 \text{ km}^3 \text{ yr}^{-1}$) and annual water discharge at Huayuankou Q_a ($0.1 \text{ km}^3 \text{ yr}^{-1}$) for the lower Yellow River from 1949 to 1957 when there was no flow regulation and the diversion was insignificant (Figure 5a):

$$Q_f = 0.6113Q_a \quad (6)$$

The second equation is an empirical relationship between Q_f and Q_{bfa} , a companion equation of Equation (5) from Chen *et al.* (2006):

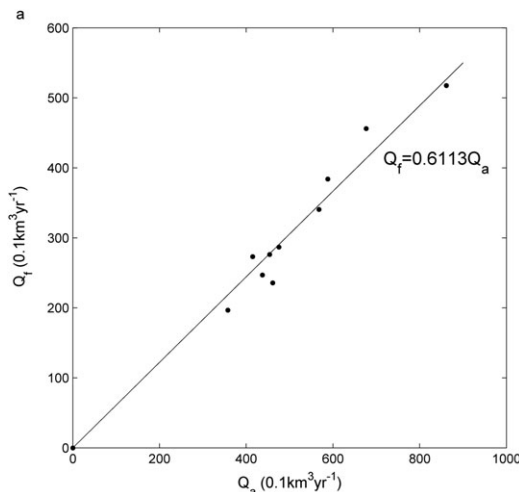


Figure 5. (a) A near-pristine correlation between water discharge in flood seasons and annual water discharge at Huayuankou for the lower Yellow River from 1949 to 1957 and in 1964. The measurement for 1964 is included to represent a record-breaking high flow year. (b) The relationship between Q_a and Q_{bfa} for the lower Yellow River between 1950 and 2003 (Chen *et al.*, 2006) and that for an ideal lower Yellow River whose water discharges experience no modern human interventions.

$$Q_{bfa} = -0.0219Q_f^2 + 26.745Q_f + 518.12 \quad (90 \leq Q_f \leq 611) \quad (7)$$

Merging the above two equations, we have the relationship between Q_a and Q_{bfa} for an ideal lower Yellow River whose water discharges experience no modern human interventions:

$$Q_{bfa} = -0.00818Q_a^2 + 16.349Q_a + 518.12 \quad (150 \leq Q_a \leq 999) \quad (8)$$

According to Equation (8), when $Q_a > 999$, Q_{bfa} decreases as Q_a increases, which is unnatural. Therefore, Q_{bfa} is extrapolated further using a linear equation with a value of slope equal to that at $Q_a = 990$:

$$Q_{bfa} = 0.1504Q_a + 8533.38 \quad (999 < Q_a \leq 1011) \quad (9)$$

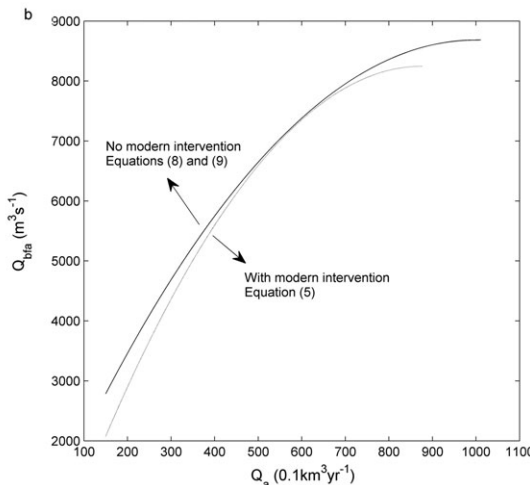
As shown in Figure 5b, if there were no river diversion and regulation, the magnitude of bankfull discharge would be larger than that calculated by Equation (5). The differences are largest when annual water discharge is very high or extremely low, which are due to intense reservoir regulations in high-flow years and substantial river diversions in the 1990s, respectively. The differences are close to 0 when Q_{bfa} ranges between 7,000 and 8,000 $\text{m}^3 \text{ s}^{-1}$. This result occurs because during the 1950s, Q_{bfa} was within this range while the Yellow River was in a near-pristine state (Chen *et al.*, 2006).

We assume that Equations (8) and (9) hold for the Old Yellow River. For non-breach years during 1580–1849, Equations (8) and (9) are used to calculate the post-flood bankfull discharge. For breach years during this period, two modified functions (Equations 10–11) are used to account for the effects of breaching, r_{oa} , on the bankfull discharge downstream from a breach:

$$Q_{bfa} = 0.00818[(1 - r_{oa})Q_a]^2 + 16.349(1 - r_{oa})Q_a + 518.12 \quad (150 \leq (1 - r_{oa})Q_a \leq 999) \quad (10)$$

$$Q_{bfa} = 0.1504(1 - r_{oa})Q_a + 8533.38 \quad (999 < (1 - r_{oa})Q_a \leq 1011) \quad (11)$$

The reduction in bankfull discharge downstream from a breach can be inferred from Equations (10) and (11). It is



evident that after a breach is repaired, the smaller bankfull discharge is a key controlling factor that shapes the occurrence of levee breaches during the impending flood season. Therefore, this post-flood bankfull discharge Q_{bf} is taken as the bankfull discharge before the flood season for the next year. Q_{bf} is further decadally averaged to yield Q_{bf} .

Figure 6 shows decadal changes in water discharge at Huayuankou Q , bankfull discharge Q_{bf} ($r_{oa}=0.45$), $\frac{Q}{Q_{bf}}$, levee conditions ($T=40$ yrs) and frequencies of levee breach events.

Uncertainty Analyses for r_{oa}

The most likely range of r_{oa} is estimated by an automatic calibration for the regression model expressed as Equation (4) (Muñeta and Nicklow, 2005; Refsgaard *et al.*, 2007; Chen *et al.*, 2015). An uncertainty analysis is employed for the calibration. First, we need to determine a likely range for r_{oa} that is as realistic as possible to guarantee an accurate calibration. As r_{oa} is mainly controlled by the long-term average duration of a breach T_b and the long-term average outflow ratio of the duration of a breach r_{ob} , we compile all relevant historical accounts of major breaches during 1580–1849 that include dates of breach initiations, breach durations, and outflow ratios of breaching flows (Supporting Material Table S1). Among the 143 breaches, 76% initiated between July and September, and the average date of initiation was mid-August. For the sake of simplification, we assume all breaches initiate on August 15. According to historical accounts, the average duration of 115 breaches was 9.1 months from their initiation date to their repair date. For the breaches that lasted for years, a new channel could form to reroute flows back to the main channel downstream (Shen *et al.*, 1935). We assume that the average duration of these breaches would be somewhat smaller, say, 8.5 months. That is, we assume all breaches are repaired on the following May 1. According to historical documents, the average outflow ratio for 40 breaches was 0.83. As people tended to record details of large events, we assume that the long-term average outflow ratio during the interval of a breach r_{ob} ranged from 0.2 to 0.8. By sampling r_{ob} at equal intervals of 0.1, we draw seven discrete likely values of r_{ob} ; that is, $r_{ob}=\{0.2, 0.3, 0.4, 0.5, 0.6, 0.7, 0.8\}$.

We further assume that long-term monthly means for water discharge during 1580–1849 were similar to those during 1949–1957 (Figure 7), when water discharge was near-pristine

and had a long-term annual mean ($57 \text{ km}^3 \text{ yr}^{-1}$) very close to those during 1580–1849 ($57.1 \text{ km}^3 \text{ yr}^{-1}$). Hence, seven discrete likely values of r_{oa} that correspond to the above seven values of r_{ob} are computed; that is, $r_{oa}=\{0.13, 0.19, 0.26, 0.32, 0.39, 0.45, 0.52\}$ for breaches that initiate on August 15 and are repaired on the following May 1 (Figure 7a).

For every likely value of r_{oa} , non-linear least squares fitting is applied to estimate the three parameters X_1 , X_2 , and X_3 in Equation (4). The performance of this fitting is evaluated by R^2 and RMSE (Willmott, 1982). R^2 measures the proportion of total variation in the observed probability of a breach explained by the fitted equation. RMSE is a measure of accuracy (Willmott *et al.*, 1985); here, it is designed to measure the average difference between predictions and observations of the decadal frequency of levee breach events.

Using R^2 and RMSE, a search algorithm is designed to identify the most likely values of r_{oa} . For the seven fitted equations corresponding to seven values of r_{oa} , the maximum value of R^2 and the minimum value of RMSE are denoted as $\max(R^2)$ and $\min(\text{RMSE})$, respectively. An equation is identified as the optimal or close-to-optimal equation when its R^2 ranges from $0.9 \max(R^2)$ to $\max(R^2)$, and meanwhile, its RMSE ranges from $\min(\text{RMSE})$ to $1.1 \min(\text{RMSE})$. The corresponding value of r_{oa} is identified as the most likely value.

Historical documents indicate that the duration of a breach T_b ranges widely from several days to 72 months (Supporting Material Table S1). To predict a full uncertainty range for r_{oa} , a second uncertainty analysis is applied to T_b to obtain the calibration values for r_{oa} when breaches are repaired on April 1 ($T_b=7.5$ months) or on June 1 ($T_b=9.5$ months) (Figure 7b, c). Uncertainty analysis is also applied to the lifetime of a levee T that determines L_v .

Constructing the Sediment Budget

We construct the sediment budget for the Old Yellow River for 1580–1849, which is decomposed into four components (Gt yr^{-1}):

$$I = S_c + S_f + O \quad (12)$$

where I is the sediment input to the Old Yellow River at Huayuankou; O is the sediment output at Yuntiguan, the apex of the delta; S_f is the sediment deposited on floodplains

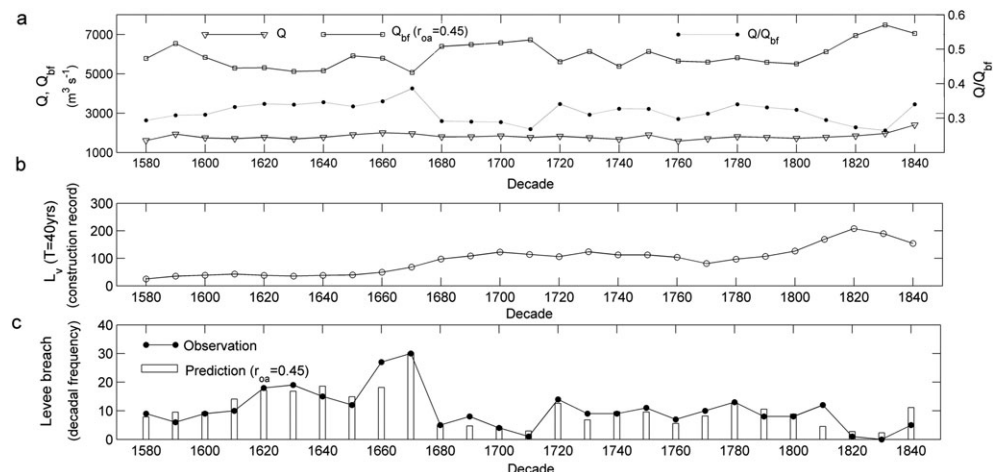


Figure 6. (a) Historical data reconstructions of decadal changes in water discharge at Huayuankou Q , bankfull discharge Q_{bf} ($r_{oa}=0.45$), and $\frac{Q}{Q_{bf}}$, (b) levee conditions and (c) frequencies of levee breach event occurrence (observation vs. prediction) on the Old Yellow River for AD 1580–1849.

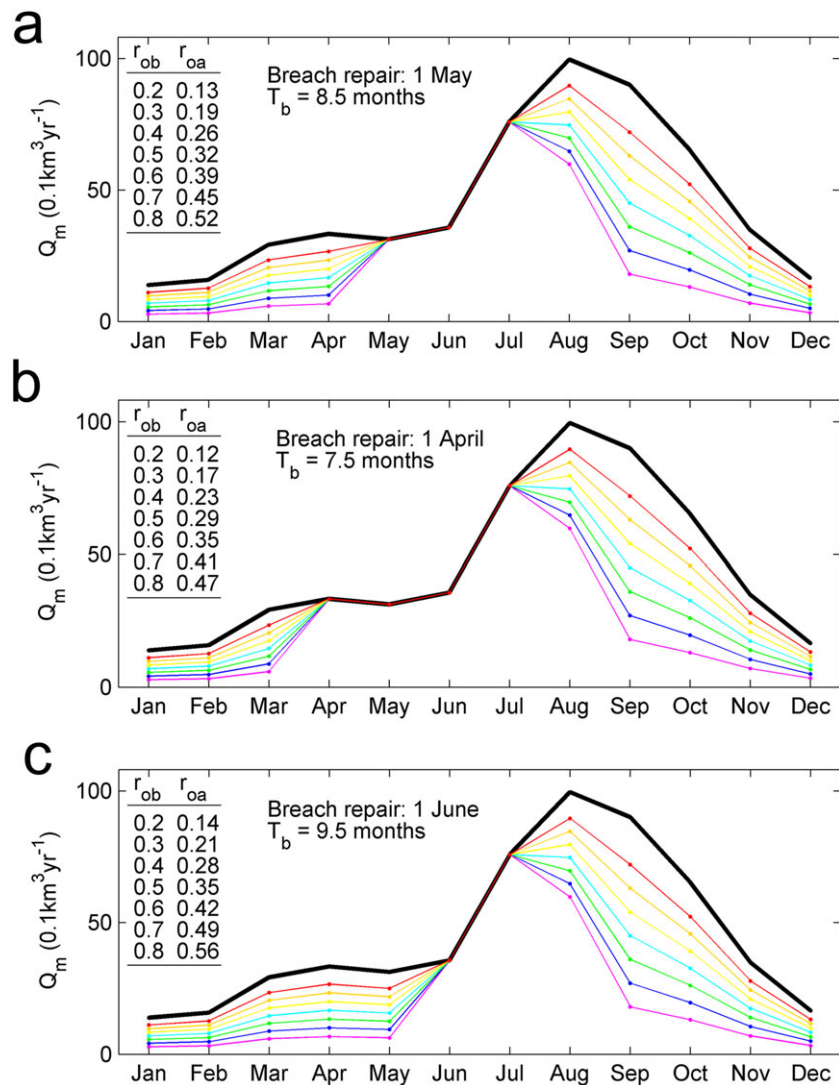


Figure 7. Long-term average monthly flow hydrographs for breaching years. Suppose breaches initiate on 15 August and can be repaired on the following (a) May 1, (b) April 1 or (c) July 1. [Colour figure can be viewed at wileyonlinelibrary.com]

outside the levees, which is estimated using the methodology described above; and S_c is the sediment flux deposited in channel belts and floodplains within the levees (Figure 2).

S_c can be approximated as follows:

$$S_c = S_{ed} LW \rho_d \quad (13)$$

where S_{ed} is the long-term average sedimentation rate within levees estimated from core data (Xu, 1998); L is the length of the channel belt, W is the average distance between two opposing levees, and both geometric parameters can be obtained from SRTM channel belt maps; and ρ_d is the dry bulk density of sediment within levees.

Results

Uncertainty Range for r_{oa}

Table I presents the fitted parameters X_1 , X_2 , and X_3 in Equation (4) and shows how the performance of the regression model changes with r_{oa} when the lifetime of a levee T is set to 40 years and the duration of a breach T_b is set to 8.5 months. Figure 8 presents how the performance of the regression model changes with r_{oa} and T_b when T is set to 40 years. For all three

T_b , as r_{oa} increases, R^2 increases, and RMSE decreases. However, both measures stabilize when r_{oa} is greater than 0.35. The search algorithm identifies the most likely value ranges of r_{oa} as 0.35–0.47, 0.39–0.52 and 0.42–0.56, for T_b values of 7.5 months, 8.5 months and 9.5 months, respectively, indicating that r_{oa} tends to increase with T_b . When T is set to 30 years or 50 years, the calibration value of r_{oa} changes to 0.39–0.56 (Supporting Material Table S2). Hence, overall, r_{oa} ranges from 0.35–0.56. Using Equation (3), R_o , the long-term average outflow ratio of breaches for 1580–1849, is found to lie between 0.188 and 0.301.

Table I. Changes in the parameters and performance of the regression model (Equation (4)) with r_{oa} and its corresponding r_{ob} for the case of $T = 40$ years and $T_b = 8.5$ months

r_{ob}	0.2	0.3	0.4	0.5	0.6	0.7	0.8
r_{oa}	0.13	0.19	0.26	0.32	0.39	0.45	0.52
X_1	147.28	636.50	835.90	243.38	34.38	7.22	1.53
X_2	6.33	7.61	8.25	7.80	6.80	5.93	5.04
X_3	-0.59	-0.60	-0.54	-0.45	-0.35	-0.29	-0.24
R^2	0.37	0.49	0.62	0.70	0.75	0.77	0.78
RMSE	5.26	4.73	4.05	3.61	3.30	3.18	3.12

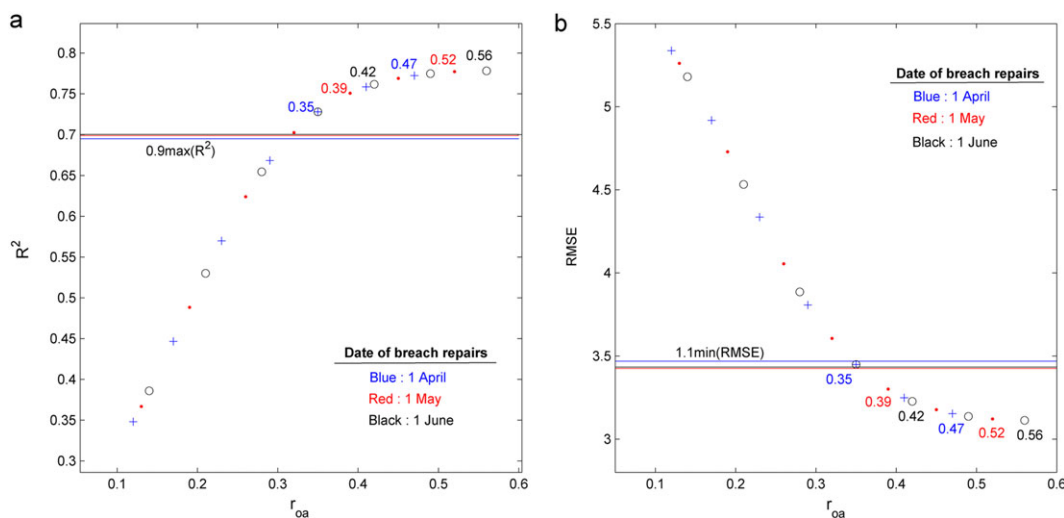


Figure 8. The performance of the regression model (Equations (6)–(8)), which is evaluated from the coefficient of determination (R^2) and the root-mean-square error (RMSE), and changes in the annual outflow ratio for breaching years r_{oa} . Optimal or near-optimal performance is achieved when r_{oa} is between 0.35 and 0.56, as $0.9 \max(R^2)$ and $1.1 \min(\text{RMSE})$ are set as the choice criteria. [Colour figure can be viewed at wileyonlinelibrary.com]

Sediment Budgets for Different Historical Periods

For 1580–1849, with a sediment input of 1.0–1.3 Gt yr^{-1} to the Old Yellow River (Ye *et al.*, 1983; Shi *et al.*, 2009) and an R_o of 0.188–0.301, the sediment flux supplied to floodplains outside the levees is 0.188–0.391 Gt yr^{-1} . S_c , the sediment flux deposited in channel belts and floodplains within the levees, is calculated using Equation (13). Taking $r_c = 25 \text{ mm yr}^{-1}$ (Xu, 1998), $L = 800 \text{ km}$, $W = 8.86 \text{ km}$ and $\rho_d = 1550 \text{ kg m}^{-3}$ (Shi *et al.*, 2002) yields $S_c = 0.275 \text{ Gt yr}^{-1}$. The remaining 0.424–0.781 Gt yr^{-1} sediment flux is delivered to the deltaic area and beyond.

Therefore, the total sediment input to the Old Yellow River for 1580–1849 is estimated as 270–350 Gt, of which 21.2–27.5% is deposited in the channel belt and in floodplains within levees and 18.8–30.1% is sequestered in floodplains outside the levees, leaving the remaining 42.4–60.0% to enter the delta (Table II). Our estimate for the sum percentage of S_c and S_f is 40–57.6%, which is in agreement with estimates by Ren (2015) and Ye *et al.* (1983) of 46% and 44%, respectively. However, our estimate for S_f is smaller than that by Ren (2015).

To better understand how floodplain sedimentation for the lower Yellow River basin was affected by human activities, we constructed sediment budgets for an additional three historical periods: 851–350 BC, AD 1128–1546 and AD 1950–1983 (Table II).

The 851–350 BC period was characterized by a pristine and stable Yellow River without human-accelerated erosion in the middle basin and embankment on the lower river (Chen *et al.*, 2015). Using Hydrotrend, a climate-driven hydrological model that incorporates human factors (Kettner and Syvitski, 2008), we estimate the sediment flux supplied to the lower Yellow River as 0.28 Gt yr^{-1} (Chen *et al.*, 2015). Assuming that the channel belt and natural levees had a sedimentation rate of 2 mm yr^{-1} (Xu, 1998) and that the length of the channel belt

and the distance between two opposite levees were 1500 km and 5 km, respectively, as the lower Yellow River then had three distributaries (Figure 1; Chen *et al.*, 2012), a sediment flux of 0.023 Gt yr^{-1} , or 8.3% of the sediment, was deposited in the channel belt and on the natural levees. Our model estimates that <5% of the sediment was trapped in floodplains behind the levees: the modelled outflow ratio of a major breach was only ~0.02 because the channel bed of the lower Yellow River was lower than its surrounding area (Chen *et al.*, 2015). Thus, in total <13.3% of the sediment was trapped in the pristine lower Yellow River Basin.

The AD 1128–1546 period was characterized by a chaotic lower Yellow River that shifted its course at least 22 times, which was due to a combination of human-induced increases in sediment discharges and no artificial levee system on the lower river (Chen *et al.*, 2012). We assume that during this period, human-accelerated erosion in the middle basin generated a sediment input of 1.0 Gt yr^{-1} to the lower Yellow River (Ye *et al.*, 1983; Shi *et al.*, 2009). As the river mouth prograded much more slowly during this period than during AD 1580–1849 (Figure 3), we infer that the channel belt close to the delta apex should have had a small sedimentation rate and that it should have been much smaller than the rate on the upper reaches of the lower Yellow River. We assume that the channel belt and levees had an average sedimentation rate of 10 mm yr^{-1} or approximately half the rate along the upper reaches of the lower Yellow River (Xu, 1998). The length of the channel belt and the distance between two opposite levees were 1200 km and 6 km, respectively, as the unconfined Yellow River then consisted of smaller distributary channels. An estimated 0.112 Gt yr^{-1} of sediment flux, or 11.2% of the sediment, was deposited in the channel belt and on the natural levees. Meanwhile, as the percentage of sediment that entered the delta during this period was undoubtedly much smaller than that for

Table II. Changes in source-to-sink sediment transfer over different periods

Period	Sediment Flux (Gt yr^{-1})				Sediment Flux (%)		
	<i>I</i>	S_c	S_f	<i>O</i>	S_c	S_f	<i>O</i>
851 B.C.–350 B.C.	0.28	0.023	<0.014	>0.243	8.3	<5.0	>86.7
A.D.1128 – A.D.1546	1.0	0.112	>>0.464	<<0.424	11.2	>>46.4	<<42.4
A.D.1580 – A.D.1849	1.0–1.3	0.275	0.188–0.391	0.424–0.781	21.2–27.5	18.8–30.1	42.4–60.0
A.D.1950 – A.D.1983	1.4	0.34	0	1.06	24.3	0	75.7

1580–1849, the percentage of sediment deposited on the floodplains outside the levees was definitely larger than that for AD 1580–1849.

The AD 1950–1983 period was characterized by intense river regulation, levee upgrades, and normalization works involving the construction of meander cutoffs and bank revetment structures. Breach outflows along the current lower Yellow River were eliminated by a levee system that was adequate to prevent breaches. As the sedimentation rate within levees jumped to 20 cm yr^{-1} (Xu, 1998), 24.3% of the sediment was trapped between levees (Table II).

Discussion

Sources of Error in Predicting r_{oa}

A regression model (Equation (4)) was used to predict r_{oa} , the annual outflow ratio r_{oa} for breach years. There are some unavoidable sources of error, such as the model inputs constructed from historical data, Q_{bf} calculated using Equations (8)–11, which are adapted from the empirical relationships for the current lower Yellow River, and the arbitrary search algorithm that causes the exclusion of the value of 0.35 from the calibration values of r_{oa} when T is set to 30 years or 50 years (Supporting Material Table S2).

To identify major sources of error in the regression model, we constructed three additional exponential regression models for breach probability using different explanatory variables Q , Q_{bf} or $\frac{Q}{Q_{bf}}$ and we compared their performances with those of Equation (4), which includes the explanatory variable for the levee condition, L_v . Table III shows that Equation (4) performs the best of the four models and can explain 78% of the total variation in observations. L_v contributes very little to its explanatory ability because after it is excluded from the set of explanatory variables, the new regression model:

$$P = X_1 \left(\frac{Q}{Q_{bf}} \right)^{X_2} \quad (14)$$

still explains 77% of the total variation in observations. This result is mostly attributed to Q_{bf} , the potential bankfull discharge of the channel before the flood season, as the regression model involving the single variable Q_{bf} :

$$P = X_1 Q_{bf}^{X_2} \quad (15)$$

is able to explain 63% of the total variation in observations. Between Equations (14) and (15), the improvement of explanatory ability is due to the addition of Q to the set of explanatory variables by constructing a variable combination $\frac{Q}{Q_{bf}}$ as a proxy for water stage. Therefore, in Equation (4), Q and Q_{bf} are the influential variables and hence are two major sources of error.

Table III. A list of four exponential regression models for the probability of levee breach based on different combinations of the explanatory variables Q , Q_{bf} , and L_v showing changes in model performance based on these models

Model	r_{oa}	$\text{max}(R^2)$	$\text{min}(\text{RMSE})$
$P = X_1 Q^{X_2}$		0.02	7.80
$P = X_1 Q_{bf}^{X_2}$	0.39–0.56	0.63	5.52
$P = X_1 (Q/Q_{bf})^{X_2}$	0.41–0.56	0.77	3.33
$P = X_1 (Q/Q_{bf})^{X_2} L_v^{X_3}$	0.35–0.56	0.78	3.11

Q is, however, less influential than Q_{bf} , but Q_{bf} is controlled by Q . Ideally, the proxy for mean stage in flood seasons $\frac{Q_f}{Q_{bf}}$ that includes water discharge in flood seasons Q_f is a more reasonable explanatory variable than $\frac{Q}{Q_{bf}}$. This difference explains the rather poor correlation found between the probability of breach occurrence and annual water discharge Q for a given year.

Equations (8)–(9) estimate Q_{bf} for an ideal lower Yellow River whose discharges experience no river diversion or regulation. However, similar to modern river diversions, breaches during 1580–1849 could have had the effect of altering the ratio of water discharge in flood seasons to annual water discharge. To examine whether Equations (8)–(9) are a rational approximation to the real relationship between Q_a and Q_{bf} for the Old Yellow River, we calculated the ratio $\frac{Q_f}{Q_a}$ for all hydrographs for breaching years used in the uncertainty analyses (Figure 7). The ratio ranges from 0.5470 to 0.6764, that is, $\pm 10\%$ from the value of 0.6113 for an ideal lower Yellow River expressed by Equation (6). For a long-term average Q_f of 332.4 ($0.1 \text{ km}^3 \text{ yr}^{-1}$), a 10% offset in Q_f can generate only a $\pm 6\%$ offset in Q_{bf} , as Equation (7) shows. We therefore assume that the error originating from the altered hydrographs during breach years is negligible for the prediction of r_{oa} .

However, the regression model (Equation (4)) has a non-negligible systematic bias, tending to over-predict when breaches are infrequent and under-predict when breaches are frequent (Figure 9). If breaches tend to be more frequent as Q increases, this bias can be caused by three factors. First, Q may be over-predicted when it decreases and under-predicted for larger discharges. Second, Q_{bf} may be under-predicted when Q decreases and over-predicted when Q becomes larger. Finally, we assume an outflow ratio equal for all breach years, regardless of how many breaches occur in a given year. However, for years with a higher breach frequency, the real outflow ratios are likely to be larger than r_{oa} , while a smaller r_{oa} results in a larger Q_{bf} and, in turn, a lower breach probability for the following year. Fortunately, as our model is designed to investigate r_o over the whole period of 1580–1849, these three sources of bias can be reduced in the long term.

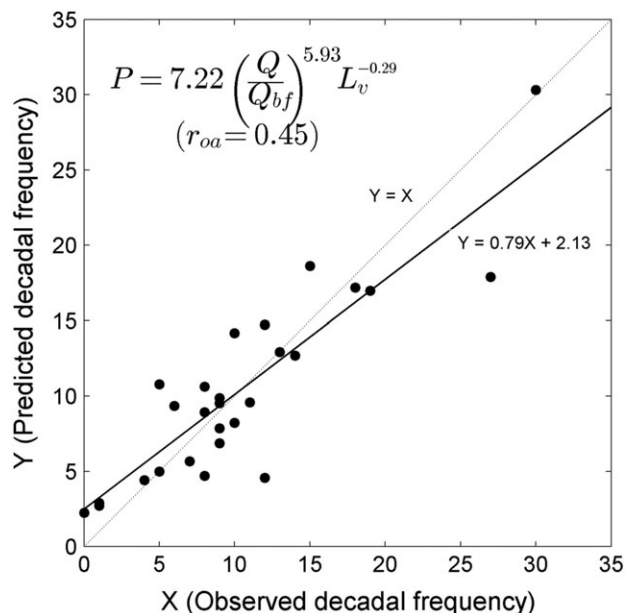


Figure 9. Scatterplots of the observed decadal frequency of levee breaches versus the predicted frequency calculated from the regression model of Equation (4) with $T = 40$ and $r_{oa} = 0.45$. The model presents a systematic bias, tending to over-predict when breaches are not frequent and under-predict when breaches are frequent.

Human-Influenced Sediment Transfer and Its Geomorphic Effects

Before the 350s BC, a pristine Yellow River existed without human-accelerated erosion in the middle basin and embankments on the lower river. As the channel belt had a sedimentation rate of approximately 2 mm yr^{-1} , it would have taken the lower river many centuries to reach its super-elevation threshold for avulsion (Chen *et al.*, 2015). The breach frequency and magnitude were very small, and <5% of the sediment was deposited on the floodplains outside the levees (Table II). Consequently, there were >180 active lakes and swamps in the extensive floodplains of the lower Yellow River [Zou, 1993]. More than 86.7% of the sediment was delivered to the delta apex. Such a high delivery ratio is reasonable, considering the fine grain size of the sediment ($\sim 0.02 \text{ mm}$) in transport (Chien and Zhou, 1965).

After AD 1128, human-accelerated erosion in the Loess Plateau had distinct off-site geomorphic implications. During AD 1128–1546, as the amount of sediment input to the lower Yellow River increased by >3 times, the sedimentation rate in the channel belt increased 10 times at the apex of the alluvial fans close to Huayuankou. As a result, the lower river became super-elevated within decades, and the breach frequency and magnitude both increased by dozens of times (Chen *et al.*, 2015). Since there was no continuous artificial levee system and few breaches were plugged, the river avulsed frequently and for many years. This period is marked by extensive sediment deposition in the floodplains outside the levees and the lowest delivery rate to the delta (Table II).

During AD 1128–1546, the lower Yellow River was not able to remain super-elevated for a long time, for it shifted its course frequently. However, during AD 1580–1849, when it was maintained along the Old Yellow River by artificial levees, sediments deposited within the levees created an ever-rising channel bed that was eventually elevated $\sim 10 \text{ m}$ above its surrounding areas by the 1850s. The high channel belt of the Old Yellow River became a drainage divide in the Huai River Basin. Distributaries in the northern basin joined the Yellow River, while the main Huai River was diverted to join the Changjiang River. The Hongze Lake rapidly expanded to an area of 2069 km^2 as the Gaojia Dike along the south-eastern lakeshore was raised to store the clear waters of the Huai River in the lake to scour the ever-rising channel bed of the Yellow River (Huai River Commission, 1990) (Figure 3).

During AD 1580–1849, the outflow ratio for the duration of a breach r_{ob} was larger than that during AD 1128–1546 (Chen *et al.*, 2015) as the super-elevation of the channel bed was beyond its threshold for avulsion. However, during AD 1580–1849, people were much more active in repairing breaches, and the breach duration decreased from several years to less than a year. Consequently, the annual outflow ratio during breach years r_{oa} decreased, and less sediment was deposited outside the levees (Table II). The sediment delivery ratio to the delta increased, resulting in a progradation rate for the river mouth that increased from $\sim 70 \text{ m yr}^{-1}$ during AD 1128–1546 to $110\text{--}1,540 \text{ m yr}^{-1}$ during AD 1580–1849. The total area of the subaerial delta and coastal plains created by the Yellow River reached $\sim 13,000 \text{ km}^2$ before the river shifted to its current course (Figure 3).

Implications for Alluvial River Management

The regression model that calculates the probability of levee breaches has implications for flood hazard management.

Equation (4) indicates that, in addition to depending on the levee condition, the probability of levee breach depends on both the water regime and channel morphodynamics, which are related to the water and sediment regimes of the river basin. River diversion and regulation reduce flood flows, leading to a narrowing of the channel and a decrease in bankfull discharge. Many global rivers, such as those in California and in the Southern Uplands of Scotland, are undergoing these anthropogenic channel changes (Gilvear *et al.*, 2002; Kondolf and Batalla, 2005) that can raise flood stages and thus exacerbate flood hazards.

Moreover, future precipitation regimes are predicted to become more unfavourable to flood defences around the globe. Modelling and observations have revealed that precipitation events will be more intense, shorter, less frequent, and less widespread in response to global warming (Giorgi *et al.*, 2014). Consequently, peak flows of rivers will change in frequency, and their magnitudes will often increase (Kettner *et al.*, 2018). As the magnitude of bankfull discharge before a flood season depends on the flow regimes of the preceding years (Pickup and Warner, 1976), a larger variability in annual water discharge means that the channel before a flood season is less likely to have an adequate discharge-carrying capacity in an impending flood event and thus more vulnerable to flood hazard. Meanwhile, the predicted precipitation regimes will exacerbate water resource scarcity for some regions, and as a result, people are very likely to increase diversions on many rivers.

Hence, flood hazard management in the future needs to develop a more holistic vision and to integrate concepts and knowledge from hydrogeomorphology (Buffin-Bélanger *et al.*, 2017). Rivers in semiarid climate zones and rivers with high sediment loads and erosive banks should be monitored more carefully in the future, for they show significant interannual variabilities in water discharge and bankfull discharge.

Changes in the sediment budget for the lower Yellow River over historical times provide implications for the construction of diversion structures, which is a common practice for floodplain restorations. The Old Yellow River, though embanked, still had an uncommonly high breach outflow ratio (r_{oa}) of 0.35–0.56 and deposited 18.8–30.1% of the sediment on the floodplains outside the levees (Table II). Regarding rivers in the Rhine Delta, after they were embanked, sediment discharges to the floodplains outside the levees decreased by an order of magnitude during AD 1300–1850 (Middelkoop *et al.*, 2010). For the embanked lower Mississippi River from AD 1880–1911, only 10% of the sediment flux to the river could be trapped behind the levees (Kesel, 1988; Kesel *et al.*, 1992).

Three conditions along the Old Yellow River favoured a high breach outflow ratio. First, the sediment composing the channel bed was dominated by fine sand and silt, which was most prone to entrainment and which thus facilitated rapid breach expansion. In comparison, riverbanks in the Rhine Delta consist predominantly of sand and gravel (Middelkoop *et al.*, 2010), and those along the lower Mississippi below the Red River consist of coarse sand or clay (Kolb, 1963).

Second, a positive feedback acted that tended to increase the frequency of breaches in the long term. As a breach on the Old Yellow River could capture a large ratio of flow, the river stream power was substantially reduced in the main channel, resulting in rapid channel aggradation downstream from the breach, which in turn increased the probability of breach occurrence in the following flood season (Chen *et al.*, 2012).

Third, super-elevation was high relative to the mean main-channel depth, or the normalized super-elevation was large. Here, we define super-elevation of a natural levee or of embanked floodplains as its relative height above adjacent

flood basins (Chen *et al.*, 2015). Normalized super-elevation controls the breach lip height, which is defined as the height of a breach throat bottom relative to the main channel depth (Slingerland and Smith, 1998). As shown in Figure 2b, the entire lower Old Yellow River had a normalized super-elevation greater than 1, suggesting that even the bed of the main channel was super-elevated and that the breach throat bottom could be lower than the bed of the main channel, thus producing a high breach outflow ratio.

The normalized super-elevation is estimated to have been ~ 3 from AD 1580–1849 on the upper reaches of the lower Yellow River, which was characterized by a braided, wide and shallow channel (Chen *et al.*, 2015). For comparison, normalized super-elevations of distributaries of the Rhine Delta and lower Mississippi River are by no means close to 3 and perhaps do not even approach 1, as denoted by cross sections in Middelkoop *et al.* (2010) and Hudson *et al.* (2008). An underlying cause is the amount of sediment input to these rivers. Levees can concentrate flows and thus shape a deeper channel with a higher sediment transport capacity. However, for the Old Yellow River, an increase in sediment input from 0.28 Gt yr^{-1} (its pristine state) to 1.2 Gt yr^{-1} was so significant that it could never have been accommodated by channel morphodynamic changes alone. As a result, sediment was deposited on both the channel bed and its floodplains within the levees at a high rate. In contrast, sediment delivered to the Rhine Delta is $<0.25\%$ of that of the Old Yellow River (Middelkoop *et al.*, 2010). Flows restricted by artificial levees should be able to carve deeper channels that can accommodate a higher sediment transport capacity; thus, the increase in normalized super-elevation can be subdued.

For the Mississippi River below the Red River from AD 1880–1911, sediment delivered to the reach was 0.71 Gt yr^{-1} , of which $\sim 7.6\%$ is estimated to have been deposited in the channel bed as upstream bank caving contributed large amounts of bedload to the reach with an $\sim 46\%$ suspended load of sand (Kesel, 1989; Kesel *et al.*, 1992). As a result, the normalized super-elevation may have increased over this period, favouring large breach outflow ratios. However, after 1963, sediment delivered to the lower Mississippi River was reduced to $\sim 0.155 \text{ Gt yr}^{-1}$ with the construction of dams in the basin and concrete revetments on the lower river, as well as a series of channel cutoffs (Kesel, 1988; Kesel, 2003). These engineered modifications were unfavourable for increasing the normalized super-elevation.

Hence, to rebuild floodplains behind levees, a diversion should preferentially be placed in an area with a high normalized super-elevation. To construct a diversion that is self-sustainable in the long run, an increasing normalized super-elevation is required to offset bed erosion upstream from the diversion. The offset can be promoted through the removal of dams and revetments upstream, through the restriction of sand mining, and through maintenance of natural meanders. In addition, a diversion should be designed with a small initial lip height to facilitate a large initial breach outflow ratio and establish a positive feedback that favours self-sustainability. A modelling study using the process-based Delft3D model has already suggested that channel aggradation downstream from a diversion structure may develop along the lower Mississippi River (Meselhe *et al.*, 2016).

Conclusions

We estimated the amount of sediment storage in the floodplains outside levees along the lower Yellow River for AD 1580–1849 using a multi-exponential regression model for the probability of levee breaches. We compiled historical accounts to obtain quantified information on the magnitudes of >100 breaches

during this period for accurate calibrations and a realistic uncertainty estimation for the breach outflow ratio. We constructed the preliminary sediment budgets for the lower Yellow River for four historical periods and summarized how floodplain sedimentation was affected by human activities over the past two millennia.

For AD 1580–1849, sediment inputs to the lower Yellow River totalled $270\text{--}350 \text{ Gt}$, of which $21.2\text{--}27.5\%$ was stored in the channel belt and floodplains within its levees, $18.8\text{--}30.1\%$ was stored in the floodplains outside the levees, and $42.4\text{--}60.0\%$ was delivered to the delta. The uncommonly high delivery ratio to the floodplains outside the levees was due to a remarkable human-induced increase in sediment delivery to the lower Yellow River. A condition favouring breach outflows was created as sediment deposition within levees generated significant super-elevation relative to the mean main channel depth. The latter should hence be considered when managing self-sustainable diversion for floodplain restoration.

Acknowledgements—Yunzhen Chen was supported by National Natural Science Foundation of China Grant 41676076 and Yellow River Institute of Hydraulic Research Grant 201801 (titled “Emergence mechanism of the alluvial river in flume experiments”). Shu Gao was supported by Ministry of Science and Technology of the People’s Republic of China Grant 2013CB956500. The data for this paper, including numbers of breaches and construction projects, are available in Supporting Material Table S1.

References

- Allen PA. 2008. From landscapes into geological history. *Nature* **451**(17 January): 274–276.
- Allison MA, Kuehl SA, Martin TC, Hassan A. 1998. Importance of flood-plain sedimentation for river sediment budgets and terrigenous input to the oceans: Insights from the Brahmaputra-Jamuna River. *Geology* **26**: 175–178.
- Bergillos RJ, Rodríguez-Delgado C, Millares A, Ortega-Sánchez M, Losada MA. 2016. Impact of river regulation on a Mediterranean delta - assessment of managed vs unmanaged scenarios. *Water Resources Research*. <https://doi.org/10.1002/2015WR018395>.
- Bracken LJ, Turnbull L, Wainwright J, Bogaart P. 2015. Sediment connectivity: A framework for understanding sediment transfer at multiple scales. *Earth Surface Processes and Landforms* **40**: 177–188. <https://doi.org/10.1002/esp.3635>.
- Buffin-Bélanger T, Demers S, Montané A. 2017. 10 - Hydrogeomorphology: Recognition and Evolution of the Flood Phenomenon A2 - Vinet, Freddy. In *Floods*. Elsevier; 167–191.
- Chen J, Hu C, Dong Z, Liu D. 2006. Change of bankfull and bed-forming discharges in the Lower Yellow River. *Journal of Sediment Research (in Chinese)* **2006**(5): 10–18.
- Chen X. 1989. Holocene sedimentation in the Huang-Huai Plains of north Jiangsu Province, China. *Journal of Stratigraphy (in Chinese)* **13**: 213–218.
- Chen Y, Overeem I, Kettner AJ, Gao S, Syvitski JPM. 2015. Modeling flood dynamics along the super-elevated channel belt of the Yellow River over the last 3000 years. *Journal of Geophysical Research - Earth Surface* **120**: 1321–1351. <https://doi.org/10.1002/2015jf003556>.
- Chen Y, Syvitski JPM, Gao S, Overeem I, Kettner AJ. 2012. Socio-economic Impacts on Flooding: A 4000-Year History of the Yellow River, China. *Ambio: A Journal of the Human Environment* **41**: 682–698.
- Chien N, Zhou W. 1965. *Channel Processes in the Lower Yellow River (in Chinese)*. Science Press: Beijing; 224.
- Day JW, Boesch DF, Clairain EJ, Kemp GP, Laska SB, Mitsch WJ, Orth K, Mashriqui H, Reed DJ, Shabman L, Simenstad CA, Streever BJ, Twilley RR, Watson CC, Wells JT, Whigham DF. 2007. Restoration of the Mississippi Delta: Lessons from Hurricanes Katrina and Rita. *Science* **315**: 1679–1684.
- Dunne T, Mertes LAK, Meade RH. 1998. Exchanges of sediment between the flood plain and channel of the Amazon River in Brazil. *Geological Society of America Bulletin* **110**: 450–467.

Esposito CR, Shen Z, Törnqvist TE, Marshak J, White C. 2017. Efficient retention of mud drives land building on the Mississippi Delta plain. *Earth Surface Dynamics* **5**: 387–397.

Florsheim JL, Dettinger MD. 2015. Promoting Atmospheric-River and Snowmelt-Fueled Biogeomorphic Processes by Restoring River-Floodplain Connectivity in California's Central Valley. In *Geomorphic Approaches to Integrated Floodplain Management of Lowland Fluvial Systems in North America and Europe*, Hudson PF, Middelkoop H (eds). Springer: New York; 321–336.

Florsheim JL, Mount JF. 2002. Restoration of floodplain topography by sand-splay complex formation in response to intentional levee breaches, Lower Cosumnes River, California. *Geomorphology* **44**: 67–94.

Gilvear DJ, Heal KV, Stephen A. 2002. Hydrology and the ecological quality of Scottish river ecosystems. *Science of the Total Environment* **294**: 131–159.

Giorgi F, Coppola E, Raffaele F. 2014. A consistent picture of the hydroclimatic response to global warming from multiple indices: Models and observations. *Journal of Geophysical Research-Atmospheres* **119**: 11,695–11,708.

Goodbred SL, Kuehl SA. 1999. Holocene and modern sediment budgets for the Ganges-Brahmaputra river system: Evidence for highstand dispersal to flood-plain, shelf, and deep-sea depocenters. *Geology* **27**: 559–562.

Gregory KJ. 2006. The human role in changing river channels. *Geomorphology* **79**: 172–191.

Huai River Commission. 1990. *A Brief History of the Huai River Conservation (in Chinese)*. China Water & Power Press: Beijing.

Hudson PF, Middelkoop H, Stouthamer E. 2008. Flood management along the Lower Mississippi and Rhine Rivers (The Netherlands) and the continuum of geomorphic adjustment. *Geomorphology* **101**: 209–236.

Kesel RH. 1988. The Decline in the Suspended Load of the Lower Mississippi River and its Influence on Adjacent Wetlands. *Environmental Geology and Water Sciences* **11**: 271–281.

Kesel RH. 1989. The role of the Mississippi River in wetland loss in southeastern Louisiana, U.S.A. *Environmental Geology and Water Sciences* **13**: 183–193.

Kesel RH. 2003. Human modifications to the sediment regime of the Lower Mississippi River flood plain. *Geomorphology* **56**: 325–334.

Kesel RH, McGraw M. 2015. The Role of Floodplain Geomorphology in Policy and Management Decisions along the Lower Mississippi River in Louisiana. In *Geomorphic Approaches to Integrated Floodplain Management of Lowland Fluvial Systems in North America and Europe*, Hudson PF, Middelkoop H (eds). Springer: New York; 321–336.

Kesel RH, Yodis EG, McCraw DJ. 1992. An approximation of the sediment budget of the lower Mississippi River prior to major human modification. *Earth Surface Processes and Landforms* **17**: 711–722.

Kettner AJ, Cohen S, Overeem I, Fekete BM, Brakenridge GR, Syvitski JJP. 2018. Estimating Change in Flooding for the 21st Century Under a Conservative RCP Forcing: A Global Hydrological Modeling Assessment. In *Global Flood Hazard: Applications in Modeling, Mapping and Forecasting*, Schumann GJ-P, Bates PD, Apel H, Aronica GT (eds). John Wiley & Sons, Inc.

Kettner AJ, Syvitski JPM. 2008. HydroTrend v.3.0: A climate-driven hydrological transport model that simulates discharge and sediment load leaving a river system. *Computers & Geosciences* **34**: 1170–1183.

Kolb CR. 1963. Sediments Forming the Bed and Banks of the Lower Mississippi River and Their Effect on River Migration. *Sedimentology* **2**: 227–234.

Kondolf GM, Batalla RJ. 2005. Hydrological effects of dams and water diversions on rivers of Mediterranean-climate regions: examples from California. In *Catchment Dynamics and River processes: Mediterranean and Other Climate Regions*, Garcia C, Batalla RJ (eds). Elsevier: The Netherlands; 197–211.

Lewin J, Ashworth PJ, Strick RJP. 2017. Spillage sedimentation on large river floodplains. *Earth Surface Processes and Landforms* **42**: 290–305.

Ma G, Wang X, Li H. 1997. *The Engineering Geology of the Lower Yellow River Course and the Quaternary Erosion of the Middle Yellow River (in Chinese)*. The Yellow River Water Conservancy Press: Zhengzhou.

Meselhe EA, Sadid KM, Allison MA. 2016. Riverside morphological response to pulsed sediment diversions. *Geomorphology* **270**: 184–202.

Middelkoop H, Erkens G, van der Perk M. 2010. The Rhine delta-a record of sediment trapping over time scales from millennia to decades. *Journal of Soils and Sediments* **10**: 628–639.

Milliman JD, Qin YS, Ren M, Saito Y. 1987. Man's influence on the erosion and transport of sediment by Asian rivers: the Yellow River (Huanghe) example. *Journal of Geology* **95**: 751–762.

Milliman JD, Syvitski JPM. 1992. Geomorphic/Tectonic Control of Sediment Discharge to the Ocean: The Importance of Small Mountainous Rivers. *The Journal of Geology* **100**: 525–544.

Milliman JD, Y-s Q, Park YA. 1989. Sediments and sedimentary processes in the Yellow and East China Seas. In *Sedimentary Facies in the Active Plate Margin*, Taira A, Masuda F (eds). Terra Scientific Publishing Company: Tokyo; 233–249.

Muleta MK, Nicklow JW. 2005. Sensitivity and uncertainty analysis coupled with automatic calibration for a distributed watershed model. *Journal of Hydrology* **306**: 127–145.

Ollero A, Ibisate A, Granado D, de Asua R. 2015. Channel Response to Global Change and Local Impacts: Perspectives and Tools for Floodplain Management, Ebro River and Tributaries, NE Spain. In *Geomorphic Approaches to Integrated Floodplain Management of Lowland Fluvial Systems in North America and Europe*, Hudson PF, Middelkoop H (eds). Springer: New York; 321–336.

Pickup G, Warner RF. 1976. Effects of hydrologic regime on magnitude and frequency of dominant discharge. *Journal of Hydrology* **29**: 51–75.

Pietsch TJ, Brooks AP, Spencer J, Olley JM, Borombovits D. 2015. Age, distribution, and significance within a sediment budget, of in-channel depositional surfaces in the Normanby River, Queensland, Australia. *Geomorphology* **239**: 17–40.

Pietz DA. 2002. *Engineering the State: The Huai River and Reconstruction in Nationalist China, 1927–37*. Routledge: New York.

Refsgaard JC, van der Sluijs JP, Hojberg AL, Vanrolleghem PA. 2007. Uncertainty in the environmental modelling process-A framework and guidance. *Environmental Modelling & Software* **22**: 1543–1556.

Ren M. 1992. Human impact on coastal landform and sedimentation. *GeoJournal* **28**: 443–448.

Ren M. 2015. Sediment discharge of the Yellow River, China: past, present and future-A synthesis. *Acta Oceanologica Sinica* **34**: 1–8.

Ren M, Zhu X. 1994. Anthropogenic influences on changes in the sediment load of the Yellow River, China, during the Holocene. *The Holocene* **4**: 314–320.

Shen Y, Zhao S, Zheng D. 1935. *The Chronicle of the Yellow River (in Chinese)*, Military Committee and Resources Committee of the Republic. Nanjing: China.

Shi C, Dian Z, You L. 2002. Changes in sediment yield of the Yellow River basin of China during the Holocene. *Geomorphology* **46**: 267–283.

Shi C, Xu J, Guo L, Zhang L. 2009. Sedimentation in the lower reaches and sediment yield in the upper and middle reaches of the Yellow River in the past 2600 years. *Quaternary Sciences* **29**: 116–125.

Slingerland R, Smith ND. 1998. Necessary conditions for a meandering-river avulsion. *Geology* **26**: 435–438.

Syvitski JPM, Kettner A. 2011. Sediment flux and the Anthropocene. *Philosophical Transactions of the Royal Society A* **369**: 957–975.

Tan Q. 1982. *The Historical Atlas of China (in Chinese)*, Vol. 1–8. China Cartographic Publishing House: Beijing.

Walling DE. 1983. The sediment delivery problem. *Journal of Hydrology* **65**: 209–237.

Walling DE. 2006. Human impact on land-ocean sediment transfer by the world's rivers. *Geomorphology* **79**: 192–216.

Wang G, Shi F, Zheng X, Gao Z, Yi Y, Ma G, Mu P. 1999. Natural Annual Runoff Estimation from 1470 to 1918 for Sanmenxia Gauge Station of Yellow River (in Chinese). *Advances in Water Science* **10**: 170–176.

Wang Z, Wu B, Wang G. 2007. Fluvial processes and morphological response in the Yellow and Weihe Rivers to closure and operation of Sanmenxia Dam. *Geomorphology* **91**: 65–79.

Wang Z-Y, Hu S, Wu Y, Shao X. 2003. Delta processes and management strategies in China. *International Journal of River Basin Management* **1**: 173–184.

Willmott CJ. 1982. Some comments on the evaluation of model performance. *Bulletin of the American Meteorological Society* **63**: 1309–1313.

Willmott CJ, Ackleson SG, Davis RE, Feddema JJ, Klink KM, Legates DR, Odonnell J, Rowe CM. 1985. Statistics for the evaluation and comparison of models. *Journal of Geophysical Research-Oceans* **90**: 8995–9005.

Wolman MG. 1967. A cycle of sedimentation and erosion in urban river channels. *Geografiska Annaler. Series A, Physical Geography* **49**: 385–395.

Wu B. 1996. *The Geographic System of the North Jiangsu Plains in Historical Times (in Chinese)*. East China Normal University Press: Shanghai.

Wu B, Wang G, Xia J. 2008. Response of bankfull discharge and sediment load in the Lower Yellow River. *Geomorphology* **100**: 366–376.

Xu F. 1989. Evolution of the Course of the Lower Yellow River in Past History. In *Taming the Yellow River: Silt and Floods*, Brush LM, Wolman MG, Huang B-W (eds). Kluwer Academic Publishers: Dordrecht, The Netherlands; 545–555.

Xu J. 1993. A study of long term environmental effects of river regulation on the Yellow River of China in historical perspective. *Geografiska Annaler. Series A, Physical Geography* **75**: 61–72.

Xu J. 1998. Naturally and anthropogenically accelerated sedimentation in the lower Yellow River, China, over the past 13,000 years. *Geografiska Annaler. Series A, Physical Geography* **80**: 67–78.

Ye QC, Jing K, Yang YF, Chen YZ, Zhang YF. 1983. Connection of channel changes of the lower Yellow River with soil erosion on the Loess Plateau. In *Proceedings of the Second International Symposium of River Sedimentation*. Water Conservancy and Electric Power Press: Beijing; 597–607.

Zhang R. 1984. Land-forming history of the Huanghe River Delta and Coastal Plain of North Jiangsu (in Chinese). *Acta Geographica Sinica* **39**: 173–184.

Zou Y. 1993. *Historical Geography of the the Huang-huai-hai Plains (in Chinese)*. In *Anhui Education Press*. Hefei: China.

Supporting Information

Additional supporting information may be found online in the Supporting Information section at the end of the article.

Table S1: The conditions of the lower Yellow River during AD 1546 and AD 1855 when its course was along the Old Yellow River. The data are based on records of *The Chronicle of the Yellow River* [Shen et al., 1935]. Ancient Chinese documented the details of many major breaches, such as dates of breach initiations, breach durations, outflow ratios. Dates of breach initiations are according to the Chinese calendar, is about 40 days behind the Gregorian calendar.

Table S2: The performances of regression models for all the cases in the uncertainty analyses. Numbers in red are the calibration values for the outflow ratio in breach years